JOC The Journal of Organic Chemistry

Article

pubs.acs.org/joc

NMR and Computational Studies of the Configurational Properties of Spirodioxyselenuranes. Are Dynamic Exchange Processes or Temperature-Dependent Chemical Shifts Involved?

David J. Press, Nicole M. R. McNeil, Arvi Rauk, and Thomas G. Back*

Department of Chemistry, University of Calgary, Calgary, Alberta, Canada T2N 1N4

Supporting Information

ABSTRACT: Spirodioxyselenurane **4a** and several substituted analogs revealed unexpected ^{1}H NMR behavior. The diastereotopic methylene hydrogens of **4a** appeared as an AB quartet at low temperature that coalesced to a singlet upon warming to 267 K, suggesting a dynamic exchange process with a relatively low activation energy. However, DFT computational investigations indicated high activation energies for exchange via inversion through the selenium center and for various pseudorotation processes. Moreover, the NMR behavior was unaffected by the presence of water or acid catalysts, thereby ruling out reversible Se−O or benzylic C−O cleavage as possible stereomutation pathways. Remarkably, when **4a** was heated beyond 342 K, the singlet was transformed into a new AB quartet. Further computations indicated that a temperature dependence of the chemical shifts of the diastereotopic protons results in convergence upon heating, followed by crossover and divergence at still higher temperatures. The NMR behavior is therefore not due to dynamic exchange processes, but rather to temperature dependence of the chemical shifts of the diastereotopic hydrogens, which are coincidentally equivalent at intermediate temperatures. These results suggest the general need for caution in ascribing the coalescence of variable-temperature NMR signals of diastereotopic protons to dynamic exchange processes that could instead be due to temperature-dependent chemical shifts and highlight the importance of corroborating postulated exchange processes through additional computations or experiments wherever possible.

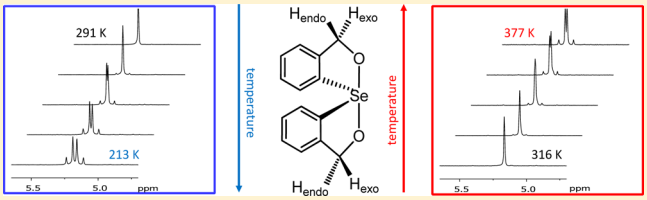

INTRODUCTION

Cyclic seleninate ester **1**[1] and spirodioxyselenurane **2**[2] (Chart 1) are highly effective catalysts for the reduction of peroxides with thiols. This property makes them of interest as mimetics[3] of glutathione peroxidase (GPx), a selenoenzyme that plays a critical role in mitigating the harmful effects of oxidative stress in the cells of higher organisms.[4] Since aromatic selenium compounds tend to be less toxic than aliphatic analogues,[3b,5] we also prepared the aromatic derivatives **3** and **4**[6,7] of **1** and **2** and evaluated their GPx activity, which can be strongly enhanced by the judicious choice of the substituent R. Our initial studies of these compounds were also extended to the diaza species **5**,[8] which contains one covalent N−Se bond and displays coordination between the selenium center and the carbonyl oxygen atom of the second amide moiety. When treated with potassium hydride in DMSO-d_6, it was transformed into the symmetrical spirodiazaselenurane dianion **6**. Subsequent work by Mugesh and co-workers[9] demonstrated that the presence of *N*-phenyl substituents results in the symmetrical diazaspiroselenurane **7**, while Singh et al. reported structural studies of related dioxy- and diazaselenuranes and related compounds.[10]

Spirodioxyselenuranes such as **2** and **4** are chiral. Stereochemical and chiroptical studies of certain related selenuranes have been reported,[11] while several such compounds have been resolved and their absolute configurations determined.[12] Other derivatives containing camphor moieties were obtained as pure diastereomers.[13] In the case of **4**, the folded structure of the molecule with respect to the central O−Se−O linkage creates

Chart 1

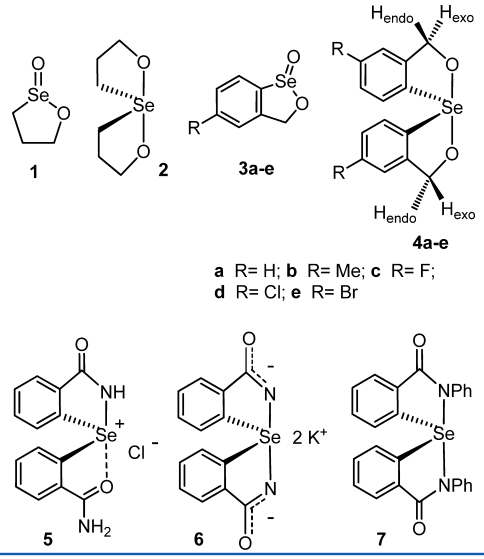

Received: August 28, 2012
Published: September 13, 2012

distinct convex and concave surfaces, with each benzylic methylene moiety containing one proton that is oriented *exo* and one that is *endo*. Consequently, the protons of each methylene group are diastereotopic, leading to the expected appearance of AB quartets in their ^{1}H NMR spectra. Although this proved to be the case for **4c**−**4e** at room temperature, the methylene signals of **4a** and **4b** were relatively sharp singlets under similar conditions. These observations suggested the possibility that the diastereotopic hydrogens of the latter were equilibrating rapidly on the NMR time scale via dynamic exchange processes with relatively low activation energies. We now report our investigation of the low-temperature NMR properties of spirodioxyselenuranes **4a**−**4e**, as well as their unexpected behavior at higher temperatures. Furthermore, computational studies of dynamic exchange processes in spirodioxyselenuranes have not yet been reported.[14] We therefore endeavored to gain further insight into the configurational stability and possible exchange processes in these compounds through a series of computational experiments. It is also worth noting that chiral cyclic seleninate esters and spirodioxyselenuranes are potential catalysts for the enantioselective oxidations of various organic substrates with stoichiometric oxidants such as hydrogen peroxide.[15] Such applications would benefit from a clearer understanding of the configurational stability of the catalysts.

RESULTS AND DISCUSSION

Dynamic NMR techniques have been successfully applied to the study of numerous types of conformational and fluxional processes, including bond rotations, inversions, racemizations, and valence isomerizations.[16] The properties of hypervalent organochalcogen compounds[17] have been subjected to numerous investigations, and several studies of exchange processes in dioxysulfuranes,[18a] tetraoxysulfuranes,[18b] dioxyselenuranes,[19a] tetraoxyselenuranes,[19b,c] and tetraoxytelluranes[19c] have been reported. Earlier NMR studies by Reich[19a] of selenuranes **8a**−**8c** revealed that **8a**, containing diastereotopic methyl substituents, was configurationally stable up to 200 °C. Moreover, diastereomers **8b** and **8c** interconverted relatively slowly at 120 °C to give the corresponding equilibrium mixture via a process that had a minimum activation energy of 30.9 kcal mol^{-1}. Related studies of sulfuranes **9a** and **9b** by Adzima and Martin[18a] indicated that the isomerization of **9a** to **9b** at 84 °C was also associated with a relatively high activation energy of 30 kcal mol^{-1}.

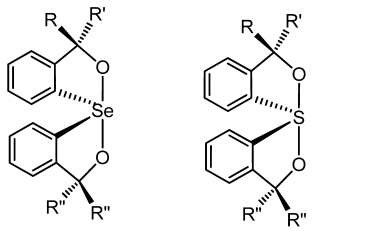

8a R, R', R'' = Me
8b R = Me; R', R'' = H
8c R' = Me; R, R'' = H

9a R, R'' = Me; R' = Et
9b R = Et; R', R'' = Me

In contrast to the behavior of **8** and **9**, **4a** and **4b** displayed singlets assigned to the methylene protons at room temperature. When the samples were cooled in toluene-d_8, the singlets separated into AB quartets. Reheating to room temperature restored the original spectra, and coalescence temperatures (T_c) of 267 and 218 K, respectively, were observed. These results indicated the presence of the respective methylene protons in distinct *exo* and *endo* environments at low temperature and their rapid interconversion at room temperature, in turn suggesting an exchange process with a relatively low activation energy. The halo-substituted derivatives **4c**−**4e** displayed the expected AB quartets at room temperature, but heating in toluene-d_8 resulted in coalescence to singlets at temperatures of 325, 355, and 370 K, respectively. Again, the process was reversible, and cooling the samples back to room temperature regenerated the original spectra. Thus, the electron-donating methyl group of **4b** decreased T_c, while the electron-withdrawing halogen substituents in **4c**−**4e** increased it, relative to the unsubstituted compound **4a**. Other solvents that were investigated for **4a** included pyridine-d_5, DMSO-d_6, and 25% D_2O−DMSO-d_6, which resulted in T_c values of 299, 347, and 368 K, respectively.

The values of T_c, $\Delta\nu$, and J for the signals of the methylene protons of **4a**−**4e** are provided in Table 1, and the variable-temperature ^{1}H NMR spectra of the unsubstituted analogue **4a** in toluene-d_8 are shown in Figure 1. The full-width variable-temperature spectra for **4a**−**4e** are provided in the Supporting Information.

Table 1. Variable-Temperature ^{1}H NMR Data for 4a−4e

compd	R	solvent	T_c (K)	$\Delta\nu^a$ (Hz)	$\lvert J_{AB}\rvert^a$ (Hz)
4a	H	toluene-d_8	267	23.4	14.6
4a	H	pyridine-d_5	299	15.6	15.6
4a	H	DMSO-d_6	347	21.0	15.0
4a	H	25% D_2O−DMSO-d_6	368	21.0	15.0
4b	Me	toluene-d_8	218	17.4	14.7
4c	F	toluene-d_8	325	19.1	14.9
4d	Cl	toluene-d_8	355	23.0	14.9
4e	Br	toluene-d_8	370	23.1	14.7

[a]Measured at the lowest temperature.

To account for the apparent rapid equilibration of the diastereotopic protons of selenuranes **4**, we considered several possible dynamic exchange mechanisms, including (1) direct inversion through the selenium center, (2) Berry pseudorotation and related processes such as the Ugi turnstile mechanism, (3) reversible dissociation of Se−O or benzylic C−O bonds.

The inversion mechanism was previously considered by Reich[19a] and by Adzima and Martin[18a] for selenuranes and sulfuranes, in which the inversion of the lone pair through a planar transition state results in enantiomerization. In the case of spirodioxyselenuranes **4**, such inversion would result in the interchange of *exo* and *endo* positions of the diastereotopic hydrogens (Scheme 1). Calculations on **4a** and the corresponding planar transition state **10a** were then conducted using the Gaussian 09 package,[20] employing the B3PW91 hybrid DFT exchange-correlation functional[21] with the 6-31+G(d,p) Pople basis set,[22] for geometry optimizations and frequency calculations. This methodology was shown to be reliable for energy and geometry calculations for selenium-containing compounds.[23] Single-point energies were also obtained at the B3PW91/6-311++G(3df,3pd) and MP2/6-311+G(2d,2p) levels of theory (for computational details, see the Experimental Section and Supporting Information). The results indicated that the difference in Gibbs free energy (ΔG_{298}) between **4a** and **10a** was 43.7 kcal mol^{-1} (Figure 2 and Table S1 in the Supporting Information), effectively ruling out rapid exchange on the NMR time scale by this mechanism to account for the observed coalescence of the AB quartet of **4a** at the relatively low temperature of 267 K (in toluene-d_8).

dx.doi.org/10.1021/jo301846a | J. Org. Chem. 2012, 77, 9268−9276

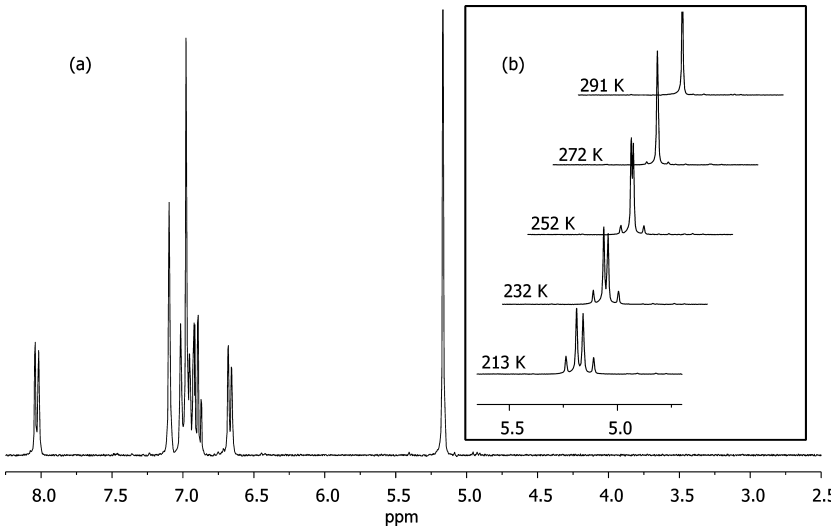

Figure 1. (a) Room-temperature and (b) variable-temperature (213−291 K) ^{1}H NMR spectra of **4a** in toluene-d_8.

Scheme 1

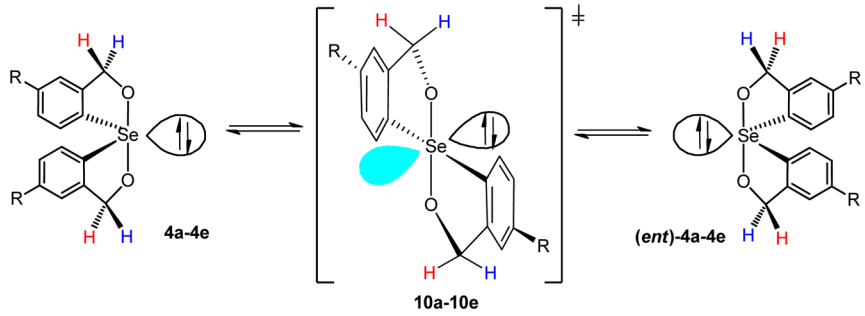

We next investigated the possibility that stereomutation by a Berry pseudorotation,[24] Ugi turnstile rotation,[25] or a similar process[26,27] is implicated in the NMR behavior of spirodioxyselenuranes **4**. Such pseudorotations are well-known in other trigonal-bipyramidal species, including those where the central atom is a chalcogen.[17b,d] Thus, Berry pseudorotation of such structures results in interconversion of the two apical substituents with two equatorial ones, while the remaining substituent remains fixed in an equatorial position and acts as a pivot for the process. In the present case, Berry pseudorotation would require a differentially populated two-site exchange (Scheme 2) between diastereomeric species **4** and **11**, where the lone pair would serve as the pivot. Selenurane **4** would be expected to be more stable than **11** because of the preference of electronegative atoms such as oxygen to occupy apical positions in trigonal-bipyramidal structures.[28] Moreover, five-membered rings in such structures are most stable when they bridge one apical and one equatorial site.[19a,28c] The pseudorotation would therefore disrupt this favored geometry, thereby increasing the energy difference between **4** and **11**. Furthermore, pseudorotation effected by pivoting around a C−Se bond in **4** would place a carbon atom and the lone pair in apical positions, again resulting in species of considerably higher energy.[19a] Similar objections apply to the stereomutation of **4** by the Ugi turnstile mechanism. Not surprisingly, separate signals that could be assigned to **11a−11e** were not detected during the variable-temperature NMR experiments conducted with **4a−4e**. These considerations argue against the mechanism in Scheme 2. On the other hand, pseudorotations have been proposed for selenurane **12** and tellurane **13**, where all four substituents of the central chalcogen atom are carbon atoms and the exchange process is fluxional.[29]

Scheme 2

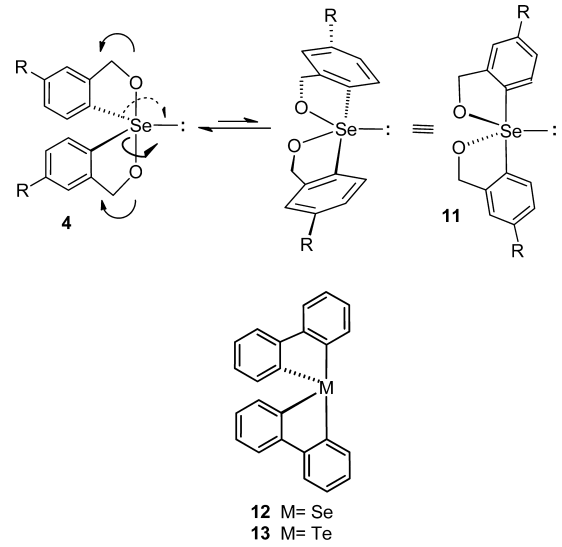

In terms of the overall transformation, Berry pseudorotations and turnstile mechanisms are equivalent.[27a,30] Moreover, for perfect trigonal-bipyramidal structures, these processes proceed via a common square-pyramidal intermediate known as the

dx.doi.org/10.1021/jo301846a | J. Org. Chem. 2012, 77, 9268−9276

"effective monkey saddle point".[31] The geometry of **4a** comprises a distorted trigonal bipyramid (if the selenium lone pair is considered as an equatorial substituent), and we attempted to determine the lowest energy pathway for potential stereomutations by means of DFT computations at the B3PW91/6-31+G(d,p) level.[20,21] The resulting profile is shown in Figure 2 and follows a path that more closely resembles a variation proposed by Meutterties,[26] instead of the classical Berry pseudorotation or Ugi turnstile mechanism. Thus, the first transition state **14** with ΔG_{298} = 32.8 kcal mol^{-1} relative to **4a**, led to a pseudo-square-pyramidal intermediate, **15** (ΔG_{298} = 19.9 kcal mol^{-1}). A second step with a transition state, (*ent*)-**16** (ΔG_{298} = 55.1 kcal mol^{-1}), then afforded the enantiomer (*ent*)-**4a** of the starting selenurane to complete the transformation. When the latter product was treated similarly, the mirror image pathway via the intermediate (*ent*)-**15** regenerated the starting material **4a** (Figure 2). The interconversion of generic structures representing **4** via this pathway is further illustrated in Scheme 3. These computations indicate that the modified pseudorotation/turnstile mechanism comprises a relatively high energy pathway with a second transition state that is even higher (ΔG_{298} = 55.1 kcal mol^{-1} relative to **4a**) than that of transition state **10** encountered in the inversion process (ΔG_{298} = 43.7 kcal mol^{-1} relative to **4a**). Thus, neither mechanism provides a viable exchange process for spirodioxyselenurane **4a** at relatively low temperatures. It is worth noting that enantiomerization by all paths in Figure 2, except inversion through **10**, involves only chiral structures. Indeed, as far back as 1954, Mislow described the possibility of enantiomerization without passing through an achiral structure.[32]

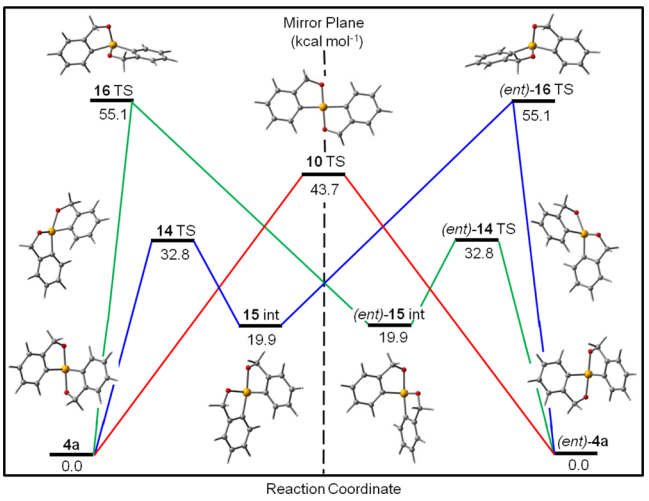

Figure 2. Potential energy surface (PES) for configurational inversion of the aromatic spirodioxyselenurane **4a**, as determined by the B3PW91/6-31+G(d,p) method (ΔG_{298} in kilocalories per mole).

Scheme 3

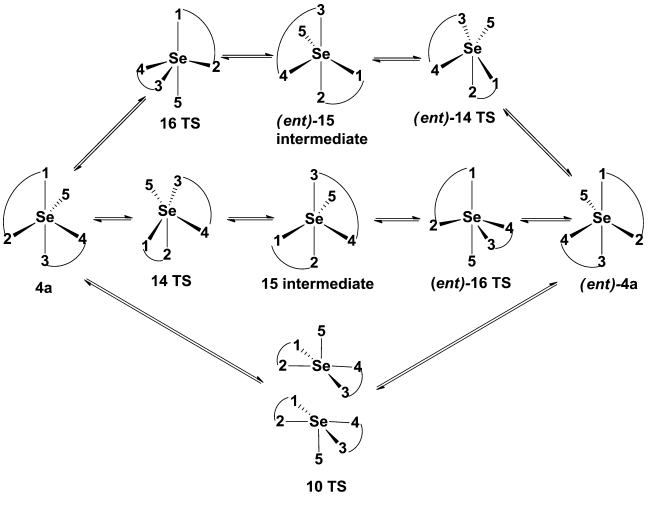

Scheme 3. These computations indicate that the modified pseudorotation/turnstile mechanism comprises a relatively high

An alternative exchange mechanism could ensue from the reversible dissociation of a Se−O bond in selenuranes **4**. Similar dissociations have been postulated in the pyrolyses of spirodioxysulfuranes[18a] and in variable-temperature NMR studies of spirotetraalkoxyselenuranes.[19c] In the presence of traces of water, this could lead to enantiomerization via the achiral selenoxide **17**. Alternatively, under anhydrous conditions, dissociation accompanied by pyramidal inversion of the resulting selenonium ion **18**,[33] or by rotation of the benzyl alkoxide moiety prior to reclosure, would also lead to enantiomerization (Scheme 4). The

Scheme 4

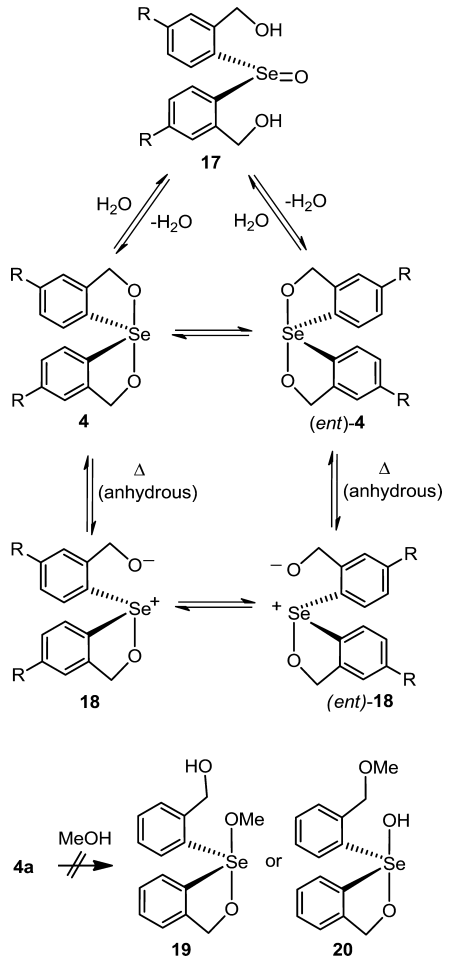

formation of intermediate **18** would be consistent with the substituent effects indicated in Table 1, as electron-donating groups *para* to the selenium atom would stabilize the development of its positive charge en route to **18**, while electron-withdrawing groups would be expected to destabilize the intermediate and retard its formation. However, neither the

dx.doi.org/10.1021/jo301846a | J. Org. Chem. 2012, 77, 9268−9276

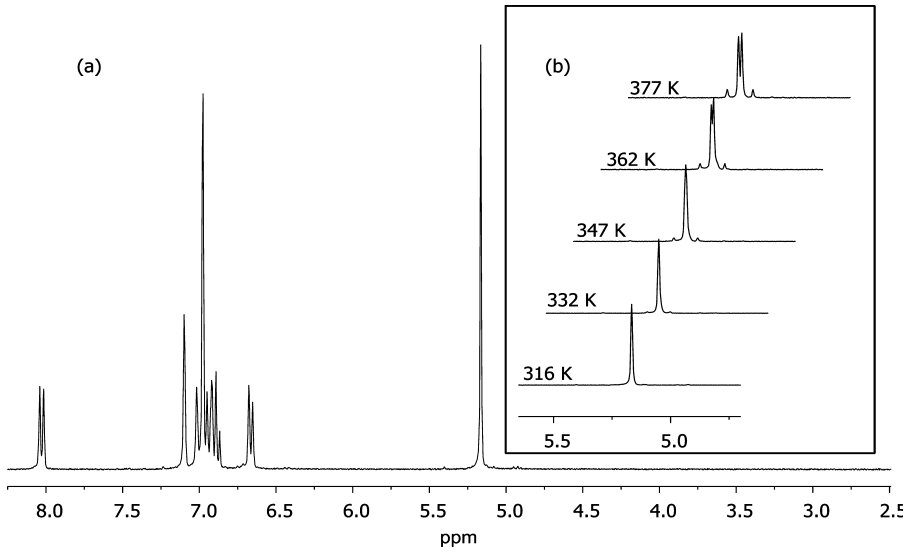

Figure 3. (a) Room-temperature and (b) variable-temperature (316−377 K) ^{1}H NMR spectra of **4a** in toluene d_8.

use of rigorously dried toluene-d_8 nor that of toluene-d_8 saturated with D_2O had any significant effect on the coalescence temperature in the variable-temperature NMR spectra of **4a**, indicating that hydrolysis does not play a role in this phenomenon. To test this possibility further, we repeated the variable-temperature studies of **4a** (T_c = 267 K in toluene-d_8) in other media, with the expectation that more polar solvents would promote Se−O dissociation. Surprisingly, in pyridine-d_5, DMSO-d_6, and 25% D_2O−DMSO-d_6, the coalescence temperatures actually increased to 299, 347, and 368 K, respectively (see Table 1). Moreover, acid catalysis would be expected to promote Se−O dissociation by initial protonation of an oxygen atom in **4a**, but no decrease in T_c was observed when catalytic amounts of trifluoroacetic acid were added to **4a** in toluene-d_8. A related mechanism involving dissociation of a benzylic C−O bond seems equally unlikely for similar reasons and because of the relatively high energy required for heterolytic cleavage of the C−O bond (ΔH_o = 91.2 kcal mol^{-1}; see Table S1 in the Supporting Information). Attempts to trap selenonium or benzylic cation intermediates by heating **4a** in methanol to afford **19** or **20**, respectively, resulted only in recovered starting material.

These experiments suggest that inversion, variations of pseudorotation, nor Se−O or C−O bond cleavage provides a satisfactory explanation for the NMR behavior of spirodioxyselenurane **4a**, due to the high activation energies of all of these pathways. A final hypothesis was based on the possibility of temperature-dependent chemical shifts[34] of the diastereotopic *exo* and *endo* protons of selenuranes **4**. In this scenario, we envisaged the gradual convergence of their respective chemical shifts with increasing temperature, resulting in the observed coalescence of their low-temperature AB quartets to singlets. Further heating could then be followed by crossover and continued divergence of their chemical shifts. To test this possibility, we heated compounds **4a** and **4b** in toluene-d_8 beyond their coalescence temperatures and observed the gradual reappearance of AB quartets at 342 and 316 K, respectively, consistent with this hypothesis. Similar high-temperature AB quartets failed to appear in the spectra of compounds **4c**−**4e**, but this is attributed to the inability to heat these samples sufficiently above their initial coalescence temperatures in toluene-d_8. The variable-temperature ^{1}H NMR spectrum of **4a** above room temperature is shown in Figure 3, while the full-width variable high temperature spectra for **4a**−**4e** are provided in the Supporting Information. Variable-temperature ^{13}C and ^{77}Se NMR experiments with **4a** revealed no new signals or other unusual behavior, while the ^{1}H NMR spectra showed no significant concentration dependence, thereby ruling out associative phenomena.

To confirm the hypothesis of temperature-dependent chemical shifts of spirodioxyselenurane **4a**, additional computations were carried out. The stationary average structure of spirodioxyselenurane **4a** has C_2 symmetry with two equivalent *exo* protons and two equivalent *endo* protons. At the vibrationless minimum on the Born−Oppenheimer (B−O) surface, the chemical shift difference $\Delta\delta_{AB}$ between diastereotopic *endo* and *exo* protons A and B, respectively, is given by $\Delta\delta_{AB} = \delta_A - \delta_B$ = 5.4816 − 5.4520 = 0.0296 ppm. The absolute calculated chemical shift values are about 0.25 ppm higher than the experimentally observed chemical shifts of ca. 5.2 ppm, but the calculated B−O chemical shift difference is smaller than that observed at 220 K (ca. 0.05 ppm) and larger than the value at 370 K (ca. 0.02 ppm).

Spirodioxyselenurane **4a** has several low-frequency, high-amplitude vibrational modes that would be significantly excited in the temperature range of the present study (Table 2). The vibrational energy levels of each of the modes are populated on the basis of Boltzmann's distribution. The resulting NMR spectrum is therefore the Boltzmann-averaged sum of the contributions of each of the vibrational modes and combinations thereof. It is important to note that vibrational modes with a_1 symmetry preserve the equivalence of the two *endo* protons, but vibrational modes with a_2 symmetry render them nonequivalent with respect to chemical shifts. The same is true of the two *exo* protons. We will refer to the chemical shifts of the *endo* and *exo* protons as the simple average of the corresponding nonequivalent chemical shifts.

If $\delta(R_q)$ is the calculated chemical shift of a particular proton at geometry R_q, where R_q is a displacement along a normal mode q with nuclear wave function $\Phi(R_q)$, then the contribution to the observed chemical shift due to normal mode q is the integrated average $\langle\Phi(R_q)|\delta(R_q)|\Phi(R_q)\rangle$. In the case of a harmonic normal mode, the classical turning points for a particular excitation level n of normal mode q with frequency ν_q, R_{qn}^{+}, and R_{qn}^{-} are points where the B−O energy is equal to $(n + 1/2)\nu_q$. This is approximately true in the case of anharmonic motion as well. We approximate the integrated average as the weighted average of the chemical shifts calculated at the two classical turning points,

dx.doi.org/10.1021/jo301846a | J. Org. Chem. 2012, 77, 9268−9276

Table 2. Vibrational Modes 1−7 of Spirodioxyselenurane 4a with the Corresponding Frequencies and Energy Levels

vibrational mode	frequency ν (cm^{-1})	symmetry	energy level (kcal mol^{-1})
1	46.02	a_1	0.069
	(0.138 kcal mol^{-1})		0.207
			0.345
			0.483
			0.621
			0.759
2	57.33	a_1	0.086
	(0.172 kcal mol^{-1})		0.258
			0.430
			0.602
			0.774
			0.946
3	103.18	a_2	0.150
	(0.310 kcal mol^{-1})		0.465
			0.775
			1.085
4	138.93	a_2	0.210
	(0.417 kcal mol^{-1})		0.417
5	185.01	a_1	0.280
	(0.560 kcal mol^{-1})		0.560
6	215.11	a_2	0.311
	(0.622 kcal mol^{-1})		0.622
			0.933
7	221.72	a_2	0.321
	(0.641 kcal mol^{-1})		0.641
			0.962

namely, $\delta(q,n) \approx w_n^+\delta(R_{qn}^+) + w_n^-\delta(R_{qn}^-)$, where w_n^+ and w_n^- are the normalized fractions of the square of the nuclear wave function that are at the isoenergetic points R_{qn}^+ and R_{qn}^-, respectively, on the potential curve. The observed chemical shift will be the sum over all normal modes and all excitation levels, weighted by the Boltzmann factor, $\exp(-n\nu_q/kT)$. In the case of a highly harmonic mode, $w_n^+ \approx w_n^- = 1/2$ for all vibrational levels (Figure 4a), little temperature dependence is expected unless the

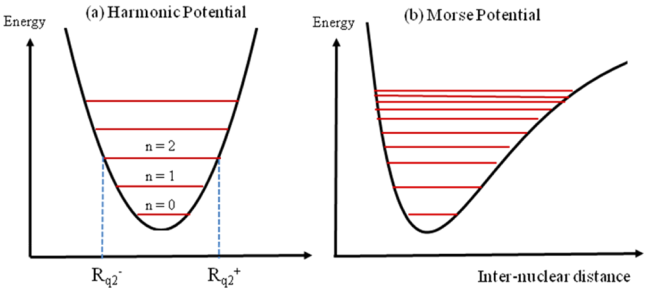

Figure 4. (a) Graphical representation of the harmonic potential. (b) Graphical representation of the Morse potential.

variation of the chemical shift, $\delta(R_q)$, is itself asymmetric (i.e., $\delta(R_{qn}^+) \neq |\delta(R_{qn}^-)|$) along the reaction coordinate. In such a case, temperature dependence of the chemical shift will arise as higher vibrational levels are populated. Temperature dependence is also expected if the particular normal mode is significantly anharmonic, such as a Morse potential, where $w_n^+ \neq w_n^-$, and the difference between w_n^+ and w_n^- will increase for higher excitation levels (Figure 4b).

To investigate the hypothesis that the observed temperature dependence of the *endo* and *exo* protons arises from anharmonicities in the vibrational normal modes or nonlinearities of $\delta(R_q)$, the calculated vibrational modes 1−7 were considered, since these will have at least one excited level that may be populated significantly at our highest temperature of 370 K.

The classical turning points, where the energy is equal to $(n + 1/2)\nu$, were located for each vibrational mode, for all energy levels populated by at least 90% according to the Boltzmann distribution (see Table S2 in the Supporting Information). As the temperature increases, higher vibrational levels can be populated, and this contribution is significant for low-frequency vibrational modes such as mode 2.

Plots of the vibrational modes (Figure 5; see the Experimental Section for computational details) revealed that only one mode,

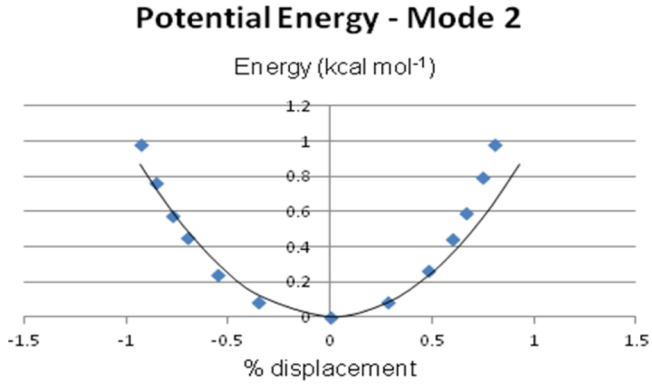

Figure 5. Energy at the classical turning points for mode 2 (tilted squares) superimposed on the harmonic potential (line).

q = 2 (a_1 symmetry), shows significant anharmonicity of the potential energy curve. We note that this fact by itself does not imply that the chemical shifts will be temperature dependent, since the NMR instrument will only record the average of the positive and negative values. However, in the case of mode 2, the anharmonicity will ensure that one side will be weighted more than the other and the balance will shift as higher vibrational modes become populated at higher temperatures. All other vibrational modes investigated were harmonic but demonstrated nonlinearity of the chemical shift for the *endo* and *exo* protons (see Figure S22 in the Supporting Information).

Figures 5 and 6 illustrate that vibrational mode 2 is lower on the negative side, such that $w_n^- > w_n^+$, and the weighting to the negative side will be higher for higher levels. We note also that the calculated chemical shift difference between *endo* and *exo* protons (designated A and B, respectively), $\Delta\delta_{AB} = \delta_A - \delta_B$, is negative on the negative side and positive on the positive side and that the averaged value of δ_{AB} is positive for the lowest vibrational level (for which $w_n^+ \approx w_n^-$). The chemical shift difference will shift from positive to negative as higher levels are populated. Specifically, if the weight w_n^- increases linearly from $w_0^- = 0.5$ to $w_5^- = 0.65$, the Boltzmann-averaged chemical shift changes from $\delta_{AB} = +0.0032$ ppm at 220 K to $\delta_{AB} = -0.0021$ ppm at 370 K and is zero at 295 K.

Thus, consideration of thermal excitations of only one mode, q_2, illustrates that vibrational motion along an anharmonic mode may result in the reversal of the signs of the chemical shift difference of diastereotopic protons and therefore the reappearance of an AB coupling pattern above the apparent coalescence

dx.doi.org/10.1021/jo301846a | J. Org. Chem. 2012, 77, 9268−9276

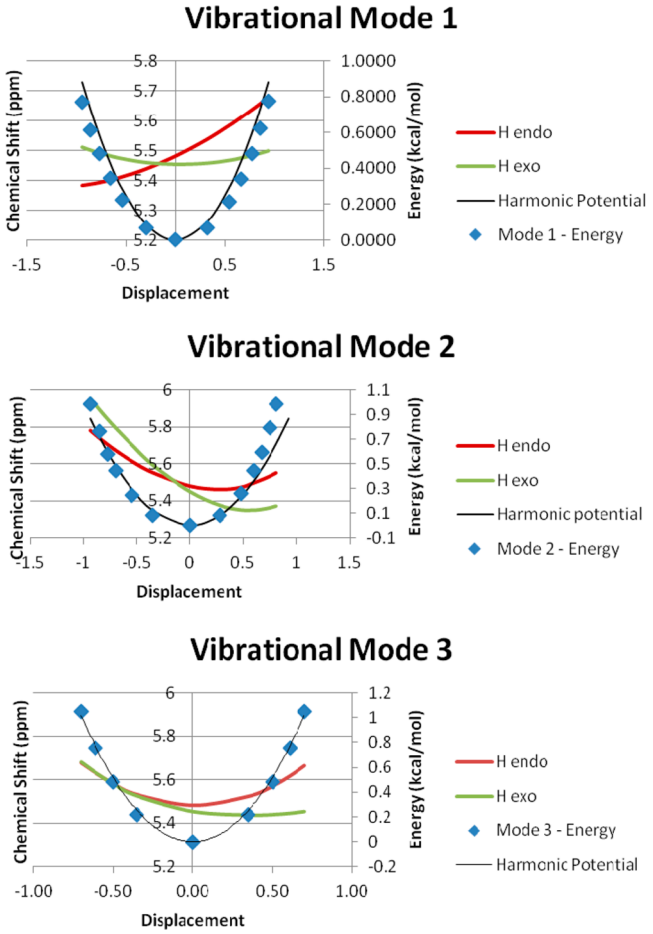

Figure 6. Overlay of the energy and harmonic potential for H_{exo} and H_{endo} in vibrational modes 1−3.

temperature. The actual calculated values are smaller than those observed. This may be the result of inaccuracies in the computational methods, and/or it may be due to the fact that combination modes such as $q_1 + q_2$ would also be populated as the temperature is raised. If multiple modes are simultaneously excited, the mapping of the geometry dependence of the calculated chemical shifts becomes a multidimensional problem of considerably greater complexity.

Once the potential energy surfaces (PESs) for vibrational modes 1−7 were compiled, NMR calculations were conducted at each classical turning point along the PES, and the chemical shifts for the diastereotopic protons were plotted against the fraction of displacement (Figures 5 and 6, and Figure S22 in the Supporting Information). As illustrated by Figure 6 for the first three vibrational modes, the chemical shifts of the diastereotopic protons are almost equivalent at the Born−Oppenheimer minimum and cross as the geometry changes along the PES in either direction. This is in accordance with the observed experimental ^{1}H NMR spectra. All seven vibrational modes investigated demonstrate the crossing of the chemical shifts of the diastereotopic protons to some extent (for vibrational modes 4−7, see Figure S22 in the Supporting Information). This correlation between chemical shifts and contributions from different vibrational modes results in the temperature dependence of the chemical shifts observed in the experimental NMR spectra. In other words, as the temperature rises, higher vibrational levels in the low-frequency vibrational modes become more populated and contribute increasingly to the overall motion of the molecule. This impacts the electronic environment surrounding the diastereotopic protons and results in the type of NMR temperature dependence observed with the spirodioxyselenurane **4a**.

CONCLUSIONS

Spirodioxyselenuranes **4** display unusual variable-temperature NMR behavior, in which their diastereotopic methylene protons appear as expected AB quartets at low temperature, coalesce to singlets upon heating, and finally, in the case of **4a** and **4b**, regenerate new AB quartets at still higher temperature. Computational studies suggest that inversion through selenium, Berry pseudorotation, and turnstile rotation all proceed by relatively high energy pathways that are inconsistent with the observed coalescence of the low-temperature AB quartets to singlets through such exchange processes. Alternatively, reversible Se−O hydrolysis to produce achiral selenoxide intermediates or heterolytic cleavage to the corresponding selenonium species, followed by their pyramidal inversion, might account for the rapid exchange of the diastereotopic protons in the NMR spectra of **4**. However, these possibilities, as well as that of benzylic C−O cleavage, are ruled out by the lack of significant solvent effects and the negligible effects of added water and acid catalysts. Furthermore, and most important, none of these alternatives provide a satisfactory rationale for the highly unexpected reappearance of a new AB quartet at still higher temperatures that were observed for **4a** and **4b**. Finally, additional computations on **4a** revealed that the anharmonicity of the PES of low-frequency vibrational modes possessing vibrational energy levels that become populated with increasing temperatures causes convergence of the chemical shifts of the diastereotopic protons. Thus, with increasing temperature, the collapse of the AB quartets to singlets is the result of coincidental equivalence. Further heating results in crossover and divergence of the chemical shifts, which manifests itself in the appearance of new AB quartets. To our knowledge, this phenomenon has not been previously observed in spirodioxyselenuranes or in other classes of trigonal-bipyramidal compounds. Our results also suggest that caution must be exercised in attributing coalescence of NMR signals of diastereotopic protons in variable-temperature experiments to dynamic exchange processes, as temperature-dependent chemical shifts that can lead to coincidental chemical shift equivalence may be a more widespread phenomenon than is generally recognized. A prudent test when such behavior is observed, providing that the sample under scrutiny is thermally stable and low barriers are not expected, is to heat as far beyond the coalescence temperature as possible to determine whether resolution of the collapsed singlet into a new multiplet occurs.

EXPERIMENTAL SECTION

Compounds **4a**−**4e** were prepared as described previously.[6] Variable-temperature proton NMR experiments were carried out at 300 MHz on a spectrometer equipped with a compressed gas heat exchanger for higher temperatures and a liquid nitrogen evaporator for low temperatures. Temperature calibration of the controller was carried out using the temperature-dependent chemical shifts of methanol (low temperature) and ethylene glycol (high temperature).[35] Samples were prepared by dissolving 0.018 mmol of the compound in 0.5 mL of deuterated solvent. Complete variable-temperature proton NMR spectra of **4a**−**4e** in toluene-d_8 with expansions near coalescence are contained in the Supporting Information, along with similar spectra for **4a** in pyridine-d_5, DMSO-d_6, and 25% D_2O/DMSO-d_6.

All calculations were performed using the Gaussian 09 package.[20] Geometry optimizations were performed with the B3PW91 hybrid DFT

dx.doi.org/10.1021/jo301846a | J. Org. Chem. 2012, 77, 9268−9276

functional, composed of Becke's three-parameter exchange functional[21a] and the correlation functional proposed by Perdew and Wang.[21b] The 6-31+G(d,p) Pople basis set[22] was employed as it was shown to be reliable for the prediction of organoselenium geometries and energetics.[23] Transition states were located with Schlegel's synchronous transit-guided quasi-Newton (STNQ) method[36a,b] and were linked to the reactants and products by intrinsic reaction coordinate calculations.[36c,d] Frequency calculations were performed on all optimized structures at the same level of theory to confirm whether the structure was a local minimum or first-order saddle point. Single-point energy calculations were also completed for all systems at the B3PW91/6-311++G-(3df,3pd) and MP2/6-31+G(2d,2p) levels of theory.

Chemical shifts along specific vibrational modes were calculated using the B3LYP/6-311+G(2d,p) level of theory using the gauge including atomic orbitals (GIAO) formalism.[37] Medium effects were not investigated.

The intramolecular PESs corresponding to individual vibrational normal modes were calculated as follows: fractions of the displacement coordinates were added or subtracted from the standard orientation coordinates, and single-point calculations of the Born−Oppenheimer energy were carried out at each point.[38] These calculations permitted an estimate of the degree of anharmonicity of each mode and the location of classical turning points based on the frequency of the vibrational mode. Classical turning points are geometries along the normal mode on either side of the minimum where the energy is equal to $(n_{ij} + 1/2)\nu_i$, where ν_i is the vibrational frequency, estimated here as the harmonic frequency of the ith normal mode, and n_{ij} is its excitation level.

Chemical shift calculations were conducted at points along the normal mode which corresponded to the classical turning points. In this study, the first seven vibrational modes given in the Gaussian output were investigated. This cutoff was taken from Boltzmann's distribution, which suggested that any vibrational modes above the seventh would not be significantly populated within the given temperature range (ca. 210−380 K).

■ ASSOCIATED CONTENT

Supporting Information

Variable-temperature NMR spectra, tables of coordinates for calculated structures, electronic energies and enthalpies of transition states and intermediates, and chemical shift computations. This material is available free of charge via the Internet at http://pubs.acs.org.

■ AUTHOR INFORMATION

Corresponding Author

*E-mail: tgback@ucalgary.ca.

Notes

The authors declare no competing financial interest.

■ ACKNOWLEDGMENTS

We thank the Natural Sciences and Engineering Research Council (NSERC) of Canada for financial support, as well as Compute Canada and the WestGrid network for providing computing resources for this work. D.J.P. and N.M.R.M. thank both the NSERC and Alberta Innovates−Technology Futures for postgraduate scholarships. We are grateful to Professor Mark MacLachlan (University of British Columbia) for helpful discussions.

■ REFERENCES

(1) (a) Back, T. G.; Moussa, Z. *J. Am. Chem. Soc.* **2002**, *124*, 12104−12105. (b) Back, T. G.; Moussa, Z. *J. Am. Chem. Soc.* **2003**, *125*, 13455−13460.

(2) Back, T. G.; Moussa, Z.; Parvez, M. *Angew. Chem., Int. Ed.* **2004**, *43*, 1268−1270.

(3) For reviews of mimetics of GPx and other selenoenzymes, see: (a) Mugesh, G.; du Mont, W.-W.; Sies, H. *Chem. Rev.* **2001**, *101*, 2125−2179. (b) Mugesh, G.; Singh, H. B. *Chem. Soc. Rev.* **2000**, *29*, 347−357. (c) Mugesh, G.; du Mont, W.-W. *Chem.—Eur. J.* **2001**, *7*, 1365−1370. (d) Bhabak, K. P.; Mugesh, G. *Acc. Chem. Res.* **2010**, *43*, 1408−1419.

(4) (a) Epp, O.; Ladenstein, R.; Wendel, A. *Eur. J. Biochem.* **1983**, *133*, 51−69. (b) Ganther, H. E. *Chem. Scr.* **1975**, *8a*, 79−84. (c) Ganther, H. E.; Kraus, R. J. In *Methods in Enzymology*; Colowick, S. P., Kaplan, N. O., Eds.; Academic Press: New York, 1984; Vol. *107*, pp 593−602. (d) Stadtman, T. C. *J. Biol. Chem.* **1991**, *266*, 16257−16260. (e) Tappel, A. L. *Curr. Top. Cell. Regul.* **1984**, *24*, 87−97. (f) Flohé, L. *Curr. Top. Cell. Regul.* **1985**, *27*, 473−478.

(5) Nogueira, C. W.; Zeni, G.; Rocha, J. B. T. *Chem. Rev.* **2004**, *104*, 6255−6286.

(6) (a) Back, T. G.; Kuzma, D.; Parvez, M. *J. Org. Chem.* **2005**, *70*, 9230−9236. (b) Press, D. J.; Mercier, E. A.; Kuzma, D.; Back, T. G. *J. Org. Chem.* **2008**, *73*, 4252−4255.

(7) Compound **4a** and related cyclic seleninate esters were independently investigated by Singh et al.: (a) Tripathi, S. K.; Patel, U.; Roy, D.; Sunoj, R. B.; Singh, H. B.; Wolmershäuser, G.; Butcher, R. J. *J. Org. Chem.* **2005**, *70*, 9237−9247. (b) Tripathi, S. K.; Sharma, S.; Singh, H. B.; Butcher, R. J. *Org. Biomol. Chem.* **2011**, *9*, 581−587.

(8) Kuzma, D.; Parvez, M.; Back, T. G. *Org. Biomol. Chem.* **2007**, *5*, 3213−3217.

(9) Sarma, B. K.; Manna, D.; Minoura, M.; Mugesh, G. *J. Am. Chem. Soc.* **2010**, *132*, 5364−5374.

(10) (a) Selvakumar, K.; Singh, H. B.; Goel, N.; Singh, U. P.; Butcher, R. J. *Dalton Trans.* **2011**, *40*, 9858−9867. (b) Selvakumar, K.; Singh, H. B.; Goel, N.; Singh, U. P.; Butcher, R. J. *Chem.—Eur. J.* **2012**, *18*, 1444−1457.

(11) For reviews, see: (a) Drabowicz, J.; Halaba, G. *Rev. Heteroat. Chem.* **2000**, *22*, 1−32. (b) Allenmark, S. *Chirality* **2008**, *20*, 544−551.

(12) (a) Claeson, S.; Langer, V.; Allenmark, S. *Chirality* **2000**, *12*, 71−75. (b) Drabowicz, J.; Luczak, J.; Mikolajczyk, M.; Yamamoto, Y.; Matsukawa, S.; Akiba, K. *Tetrahedron: Asymmetry* **2002**, *13*, 2079−2082. (c) Drabowicz, J.; Luczak, J.; Mikolajczyk, M.; Yamamoto, Y.; Matsukawa, S.; Akiba, K. *Chirality* **2004**, *16*, 598−601. (d) Petrovic, A. G.; Polavarapu, P. L.; Drabowicz, J.; Zhang, Y.; McConnell, O. J.; Duddeck, H. *Chem.—Eur. J.* **2005**, *11*, 4257−4262. (e) Gáti, T.; Tóth, G.; Drabowicz, J.; Moeller, S.; Hofer, E.; Polavarapu, P.; Duddeck, H. *Chirality* **2005**, *17*, S40−S47. (f) Lindgren, B. *Acta Chem. Scand.* **1972**, *26*, 2560−2561.

(13) (a) Zhang, J.; Koizumi, T. *Phosphorus, Sulfur Silicon Relat. Elem.* **2000**, *157*, 225−252. (b) Zhang, J.; Takahashi, S.; Saito, S.; Koizumi, T. *Tetrahedron: Asymmetry* **1998**, *9*, 3303−3317.

(14) For NMR and computational studies of aza- and oxyselenuranes produced by oxidation of selenomethionine, see: Ritchey, J. A.; Davis, B. M.; Pleban, P. A.; Bayse, C. A. *Org. Biomol. Chem.* **2005**, *3*, 4337−4342.

(15) For a recent report on the use of related cyclic seleninate esters as catalysts for the racemic oxidations of sulfides to sulfoxides, alkenes to epoxides, and enamines to α-hydroxyketones, see: Mercier, E. A.; Smith, C. D.; Parvez, M.; Back, T. G. *J. Org. Chem.* **2012**, *77*, 3508−3517.

(16) (a) Ōki, M. *Applications of Dynamic NMR Spectroscopy to Organic Chemistry*; VCH: Weinheim, Germany, 1985. (b) Sandström, J. *Dynamic NMR Spectroscopy*; Academic Press: London, 1982. (c) Lambert, J. B.; Mazzola, E. P. *Nuclear Magnetic Resonance Spectroscopy*; Pearson-Prentice Hall: Upper Saddle River, NJ, 2004; Chapter 5.2.

(17) For reviews of tetravalent and higher valent selenium compounds, see: (a) Bergman, J.; Engman, L.; Sidén, J. In *The Chemistry of Organic Selenium and Tellurium Compounds*; Patai, S., Rappoport, Z., Eds.; Wiley: Chichester, U.K., 1986; Vol. *1*, Chapter 14. (b) Drabowicz, J.; Kielbasinski, P.; Zajac, A. In *The Chemistry of Organic Selenium and Tellurium Compounds*; Rappoport, Z., Ed.; Wiley: Chichester, U.K., 2012; Vol. *3*, Part 2, Chapter 15. (c) Drabowicz, J.; Mikolajczyk, M. In *Organoselenium Chemistry*; Wirth, T., Ed.; Springer-Verlag: Berlin, 2000; pp 143−176. (d) Sato, S.; Takahashi, O.; Furukawa, N. *Coord. Chem. Rev.* **1998**, *176*, 483−514.

(18) (a) Adzima, L. J.; Martin, J. C. *J. Org. Chem.* **1977**, *42*, 4006−4016. (b) Astrologes, G. W.; Martin, J. C. *J. Am. Chem. Soc.* **1976**, *98*, 2895−2900.
(19) (a) Reich, H. J. *J. Am. Chem. Soc.* **1973**, *95*, 964−966. (b) Denney, D. B.; Denney, D. Z.; Hsu, Y. F. *J. Am. Chem. Soc.* **1978**, *100*, 5982−5983. (c) Denney, D. B.; Denney, D. Z.; Hammond, P. J.; Hsu, Y. F. *J. Am. Chem. Soc.* **1981**, *103*, 2340−2347.
(20) Frisch, M. J.; Trucks, G. W.; Schlegel, H. B.; Scuseria, G. E.; Robb, M. A.; Cheeseman, J. R.; Scalmani, G.; Barone, V.; Mennucci, B.; Petersson, G. A.; Nakatsuji, H.; Caricato, M.; Li, X.; Hratchian, H. P.; Izmaylov, A. F.; Bloino, J.; Zheng, G.; Sonnenberg, J. L.; Hada, M.; Ehara, M.; Toyota, K.; Fukuda, R.; Hasegawa, J.; Ishida, M.; Nakajima, T.; Honda, Y.; Kitao, O.; Nakai, H.; Vreven, T.; Montgomery, J. A., Jr.; Peralta, J. E.; Ogliaro, F.; Bearpark, M.; Heyd, J. J.; Brothers, E.; Kudin, K. N.; Staroverov, V. N.; Kobayashi, R.; Normand, J.; Raghavachari, K.; Rendell, A.; Burant, J. C.; Iyengar, S. S.; Tomasi, J.; Cossi, M.; Rega, N.; Millam, J. M.; Klene, M.; Knox, J. E.; Cross, J. B.; Bakken, V.; Adamo, C.; Jaramillo, J.; Gomperts, R.; Stratmann, R. E.; Yazyev, O.; Austin, A. J.; Cammi, R.; Pomelli, C.; Ochterski, J. W.; Martin, R. L.; Morokuma, K.; Zakrzewski, V. G.; Voth, G. A.; Salvador, P.; Dannenberg, J. J.; Dapprich, S.; Daniels, A. D.; Farkas, O.; Foresman, J. B.; Ortiz, J. V.; Cioslowski, J.; Fox, D. J. *Gaussian 09*, revision A.01; Gaussian, Inc.: Wallingford, CT, 2009.
(21) (a) Becke, A. D. *J. Chem. Phys.* **1993**, *98*, 5648−5652. (b) Perdew, J. P.; Wang, Y. *Phys. Rev. B* **1992**, *45*, 13244−13249.
(22) *Ab Initio Molecular Orbital Theory*; Hehre, W. J., Radom, L., von R. Schleyer, P., Pople, J. A., Eds.; John Wiley & Sons: New York, 1986.
(23) (a) Pearson, J. K.; Ban, F.; Boyd, R. J. *J. Phys. Chem. A* **2005**, *109*, 10373−10379. (b) Heverly-Coulson, G. S.; Boyd, R. J. *J. Phys. Chem. A* **2011**, *115*, 4827−4831.
(24) (a) Berry, R. S. *J. Chem. Phys.* **1960**, *32*, 933−938. (b) Whitesides, G. M.; Mitchell, H. L. *J. Am. Chem. Soc.* **1969**, *91*, 5384−5386.
(25) Ugi, I.; Marquarding, D.; Klusacek, H.; Gillespie, P.; Ramirez, F. *Acc. Chem. Res.* **1971**, *4*, 288−296.
(26) For other variations of the turnstile mechanism, see: (a) Muetterties, E. L. *J. Am. Chem. Soc.* **1969**, *91*, 1636−1643. (b) Muetterties, E. L. *J. Am. Chem. Soc.* **1969**, *91*, 4115−4122.
(27) For overviews of such processes, see: (a) Moberg, C. *Angew. Chem., Int. Ed.* **2011**, *50*, 10290−10292. (b) Cass, M. E.; Hii, K. K.; Rzepa, H. S. *J. Chem. Educ.* **2006**, *83*, 336. (c) Bürgi, H. B.; Dunitz, J. D. *Acc. Chem. Res.* **1983**, *16*, 153−161. (d) Mislow, K. *Acc. Chem. Res.* **1970**, *3*, 321−331. (e) For pseudorotations in sulfur compounds, see: Oae, S. *Organic Sulfur Chemistry: Structure and Mechanism*; CRC Press: Boca Raton, FL, 1991; pp 18−21.
(28) (a) Muetterties, E. L.; Mahler, W.; Schmutzler, R. *Inorg. Chem.* **1963**, *2*, 613−618. (b) Muetterties, E. L.; Mahler, W.; Packer, K. J.; Schmutzler, R. *Inorg. Chem.* **1964**, *3*, 1298−1303. (c) Gorenstein, D.; Westheimer, F. H. *J. Am. Chem. Soc.* **1970**, *92*, 634−644.
(29) Ogawa, S.; Sato, S.; Erata, T.; Furukawa, N. *Tetrahedron Lett.* **1992**, *33*, 1915−1918.
(30) Couzijn, E. P. A.; Slootweg, J. C.; Ehlers, A. W.; Lammertsma, K. *J. Am. Chem. Soc.* **2010**, *132*, 18127−18140.
(31) Mauksch, M.; von R. Schleyer, P. *Inorg. Chem.* **2001**, *40*, 1756−1769.
(32) (a) Mislow, K. *Science* **1954**, *120*, 232−233. (b) Mislow, K.; Bolstad, R. *J. Am. Chem. Soc.* **1955**, *77*, 6712−6713.
(33) Previous studies of the stereomutation of selenonium ions indicated relatively high barriers to pyramidal inversion, exceeding those of the corresponding sulfonium ions and suggesting that the pathway via the inversion of **18** in Scheme 4 would be unlikely at or below room temperature. See: (a) Brinkmann, T.; Uzar, H. C. *J. Chem. Soc., Perkin Trans. 2* **2000**, 527−530. (b) Wiegrefe, A.; Brinkmann, T.; Uzar, H. C. *J. Phys. Org. Chem.* **2001**, *14*, 205−209.
(34) While the temperature dependence of proton chemical shifts associated with hydrogen-bonded species is well-known, there are relatively few such studies of other types of compounds; for some examples, see: (a) Jameson, C. J. *Annu. Rev. Phys. Chem.* **1996**, *47*, 135−169. (b) Jameson, A. K.; Jameson, C. J. *J. Am. Chem. Soc.* **1973**, *95*, 8559−8561. (c) Cross, B. P.; Schleich, T. *Org. Magn. Reson.* **1977**, *10*, 82−85. (d) Hoffman, R. E.; Becker, E. D. *J. Magn. Reson.* **2005**, *176*, 87−98.
(35) (a) Ammann, C.; Meier, P.; Merbach, A. E. *J. Magn. Reson.* **1982**, *46*, 319−321. (b) Van Geet, A. L. *Anal. Chem.* **1968**, *40*, 2227−2229. (c) Van Geet, A. L. *Anal. Chem.* **1970**, *42*, 679−680.
(36) (a) Peng, C.; Ayala, P. Y.; Schlegel, H. B.; Frisch, M. J. *J. Comput. Chem.* **1996**, *17*, 49−56. (b) Peng, C.; Schlegel, H. B. *Isr. J. Chem.* **1993**, *33*, 449−454. (c) Gonzalez, C.; Schlegel, H. B. *J. Chem. Phys.* **1989**, *90*, 2154−2161. (d) Gonzalez, C.; Schlegel, H. B. *J. Phys. Chem.* **1990**, *94*, 5523−5527.
(37) Ditchfield, R. *Mol. Phys.* **1974**, *27*, 789−807.
(38) (a) Gee, C. H.; Raynes, W. T. *Chem. Phys. Lett.* **2000**, *330*, 595−602. (b) Ruud, K.; Åstrand, P.-O.; Taylor, P. R. *J. Am. Chem. Soc.* **2001**, *123*, 4826−4833. (c) Sabzyan, H.; Buzari, B. *Chem. Phys.* **2008**, *352*, 297−305.